



**CHINA** 中国地质(英文)  
**GEOLOGY**



China Geological Survey conducted the first natural gas hydrates production test in the South China Sea

## Hydrological response characteristics of landslides under typhoon-triggered rainstorm conditions

Tai-li Zhang, Ai-guo Zhou, Qiang Sun, He-sheng Wang, Jian-bo Wu, Zheng-hua Liu

**Citation:** Tai-li Zhang, Ai-guo Zhou, Qiang Sun, He-sheng Wang, Jian-bo Wu, Zheng-hua Liu, 2020. Hydrological response characteristics of landslides under typhoon-triggered rainstorm conditions, *China Geology*, 3, 455–461. doi: [10.31035/cg2020028](https://doi.org/10.31035/cg2020028).

View online: <https://doi.org/10.31035/cg2020028>

---

## Related articles that may interest you

[Progress of Deep Geological Survey Project under the China Geological Survey](#)

*China Geology*. 2020, 3(1), 153 <https://doi.org/10.31035/cg2020001>

[Temporal and spatial evolution of surface sediments characteristics in the Dagu River estuary and their dynamic response mechanism](#)

*China Geology*. 2019, 2(3), 325 <https://doi.org/10.31035/cg2018092>

[The response between glacier evolution and eco-geological environment on the Qinghai-Tibet Plateau](#)

*China Geology*. 2019, 2(1), 1 <https://doi.org/10.31035/cg2018078>

[Geological characteristics and co-exploration and co-production methods of Upper Permian Longtan coal measure gas in Yangmeishu Syncline, Western Guizhou Province, China](#)

*China Geology*. 2020, 3(1), 38 <https://doi.org/10.31035/cg2020020>

[An overview of the resources and environment conditions and major geological problems in the Yangtze River economic zone, China](#)

*China Geology*. 2018, 1(3), 435 <https://doi.org/10.31035/cg2018040>

[Deep Continental Scientific Drilling Engineering Project in Songliao Basin: progress in Earth Science research](#)

*China Geology*. 2018, 1(2), 173 <https://doi.org/10.31035/cg2018036>



## Hydrological response characteristics of landslides under typhoon-triggered rainstorm conditions

Tai-li Zhang<sup>a, b, \*</sup>, Ai-guo Zhou<sup>a</sup>, Qiang Sun<sup>b</sup>, He-sheng Wang<sup>b</sup>, Jian-bo Wu<sup>b</sup>, Zheng-hua Liu<sup>c</sup>

<sup>a</sup> Nanjing Center, China Geological Survey, Ministry of Natural Resources, Nanjing 210016, China

<sup>b</sup> China University of Geosciences, Wuhan 430074, China

<sup>c</sup> Geological Environment Monitoring Institute of Zhejiang Province, Hangzhou 310007, China

### ARTICLE INFO

#### Article history:

Received 15 September 2018  
 Received in revised form 3 January 2020  
 Accepted 17 April 2020  
 Available online 7 August 2020

#### Keywords:

Typhoon-triggered rainstorm  
 Landslide  
 Seepage  
 Hydrological response  
 Hydrogeological survey engineering  
 Geological disaster survey engineering  
 Zhejiang Province  
 China

### ABSTRACT

Many landslide disasters, which tend to result in significant damage, are caused by typhoon-triggered rainstorms. In this case, it is very important to study the dynamic characteristics of the hydrological response of landslide bodies since it enables the early warning and prediction of landslide disasters in typhoon periods. To investigate the dynamic mechanisms of groundwater in a landslide body under typhoon-triggered rainstorm conditions, the authors selected the landslide occurring in Zhonglin Village, Wencheng County, China (also referred to as Zhonglin Village landslide) as a case study. The transient seepage field characteristics of groundwater in the landslide body were simulated with two different rainfall models by using the finite element method (FEM). The research results show that the impact of typhoon-triggered rainstorms on landslides can be divided into three stages: (i) Rapid rise of groundwater level; (ii) infiltration of groundwater from the surface to deeper level, and (iii) surface runoff erosion. Moreover, the infiltration rate of groundwater in the landslide body is mainly affected by the intensity of typhoon-induced rainfall. It can be deduced that higher rainfall intensity leads to a greater potential difference and a higher infiltration rate. The rainfall intensity also determines the development mode of landslide deformation and destruction.

©2020 China Geology Editorial Office.

## 1. Introduction

Typhoons have caused a large number of geological disasters and serious destruction (Chen GP, 2011). For example, Typhoon No. 19 in 1992 led to large landslides in Lingkou Village, Xidian Town, Ninghai County, Zhejiang Province, destroying the 272 houses of 48 households. In 2004, Typhoon No. 14 (Yunna) triggered 21 geological disasters in Yueqing, Zhejiang Province, leaving 42 people dead and 288 houses collapsed (excluding damaged houses). In 2005, Typhoon Taili caused 14 landslides and 6 mudslides in Wencheng County, Wenzhou City, killing 17 people and leading to economic loss of about  $20 \times 10^6$  RMB (Han J, 2012). In 2015, Typhoon No. 13 (Suidiluo) led to 204 geological disasters in Wenzhou, causing the death of five people and economic loss of about  $28.04 \times 10^6$  RMB. As one

kind of the typhoon-induced geological disasters, landslides have received much attention of Chinese and overseas researchers because of their frequency and scale and the serious damage they cause (Han J, 2012; Chen X et al., 2007; Lou WP et al., 2006). The occurrence of landslides has been shown by research and data to be closely related to torrential rain associated with typhoons. Therefore, typhoon-triggered rainfall serves as a key factor in inducing landslides (Chen GP, 2011; Han J, 2012).

Based on a comparison and analysis of 195 landslides induced by 11 typhoons in Wenzhou City from 2004 to 2009, some researchers found that the distribution of landslide disasters were consistent with the range of typhoon-triggered rainstorms (Chen GP, 2011; Han J, 2012). These landslides mainly occurred in the areas where process rainfall was more than 200 mm or interval rainfall was more than 100 mm. They are roughly synchronized with the typhoon-triggered rainstorms without obvious hysteresis phenomena (Chen X et al., 2007). The typhoon-triggered rainstorms mainly affect the landslide slope stability through slope erosion and seepage

\* Corresponding author: E-mail address: [zhangtaili@126.com](mailto:zhangtaili@126.com) (Tai-li Zhang).

action (Zhou CB et al., 2009; Li MB et al., 2019), both of which cause the increase in the shear stress of the sliding surface, and thus the shear strength decreases (Zhang CY et al., 2019; Tang MG et al., 2019). Some part of the runoff generated from typhoon-triggered rainstorm causes erosion of the slopes and slope foot and changes the slope structure (Chen GP, 2011; Liu LL et al., 2008), while other parts of the runoff saturate the rock mass through seepage, significantly increasing the saturation. This increases the dynamic hydrostatic pressure and thereby reduces the shear strength of the rock and soil. It is a difficult research problem to determine the coupling between the runoff on the typhoon-triggered landslide slope and unsaturated seepage (Liu LL et al., 2008; Tan JM et al., 2018; Tang MG et al., 2019; Yin YP et al., 2017).

The coupling is important as it affects both the dynamic characteristics and regularity of hydrological response of landslides and also serves as the key to the assessment of slope stability and early warning and prediction of landslides (Li MB et al., 2019; Xiao SC et al., 2018; Yan YJ et al., 2019).

The landslides induced by typhoon-triggered rainstorms share similar formation mechanism with the ones caused by

general rainstorms (Fig. 1); however, the two kinds of landslides exhibit obviously different hydrological response characteristics owing to the long duration, intensity, and concentration of typhoon-triggered rainstorms (Chen GP, 2011; Qiao YX et al., 2009). In this paper, Zhonglin Village Landslide is selected as a case study to simulate different typhoon-triggered rainfall conditions and to study the dynamic characteristics of groundwater seepage of landslides. This study will enable a better understanding of the dynamic mechanisms of groundwater in the unsaturated rock mass under typhoon-triggered rainstorm conditions and will assist in the treatment and early warning and prediction of typhoon-induced landslides in the southeastern coastal areas of China.

## 2. Key characteristics of the Zhonglin Village landslide

The Zhonglin Village landslide is located to the north of Zhonglin Bridge along Provincial Highway No. 56, Wencheng County, Wenzhou City, Zhejiang Province. The slope section where the landslide occurred features a maximum elevation of 251 m at the peak position, a minimum elevation of 198 m at the foot, and a vertical height of approximately 58 m. The parameters of horizontal projection



**Fig. 1.** Photos of landslides induced by typhoon-triggered rainstorms. a—a landslide in Shuangxikou Village, Fengwen Town, Taishun County, Wenzhou City, Zhejiang Province; b—a landslide in Zhaoan City, Fujian Province; c—a landslide in Wuping City, Fujian Province; d—a landslide in Taishi Village, Taishun County, Wenzhou City, Zhejiang Province.

of the slope section are as follows: length=107 m, width=47 m, thickness=4–8 m, volume=24000 m<sup>3</sup>. The main sliding direction is 85°. The slope is gentle in the upper parts and steep in the lower parts, with a gradient of 31°–24°. Nine scarps developed.

The landslide is formed in Cretaceous strata. The landslide body consists of highly or completely weathered rock masses with spallation and fragmentation structures. As revealed from drilling exploration, the landslide body can be divided into four layers from top to bottom (Fig. 2) as follows. (1) Loose residual slope layer ( $Q_p^{edl}$ ): Yellow and brownish-yellow, comprised of breccia-bearing silty clay, 0.3–2.4 m thick, loose, and plastic. (2) Cretaceous layer ( $K_7c$ ): Brownish-yellow and grayish-brown, consisting of completely weathered tuff, 2.4–4.9 m thick. (3) Cretaceous layer ( $K_7c$ ): Grayish-yellow and grayish-brown, comprised of highly weathered tuff, 3–5.8 m thick. (4) Cretaceous layer ( $K_7c$ ): Light grey and grayish-brown, moderately weathered, comprised of tuff. The sliding surface is a highly weathered layer and the sliding zone consists of gravelly soil.

The Zhonglin Village landslide was reactivated mainly by a rainstorm that occurred on June 19th, 2012 and was associated with Typhoon No. 5 (Taili). Heavy rains of more than 200 mm/d struck Wencheng County (Xie JM et al., 2003; Wang JY et al., 2019). It changed the hydrogeological conditions of the landslide body and led to the formation of multiple tensile and shear cracks in the slope and significant deformation. Therefore, the study on the dynamic characteristics of the hydrological response of the landslide under typhoon-triggered rainstorm conditions is the key to the assessment of the slope stability.

### 3. Numerical simulation of the saturated - unsaturated seepage field of the landslide under typhoon-triggered rainstorm conditions

#### 3.1. Saturated and unsaturated seepage model of the landslide

The soil in a landslide body changes from unsaturated to saturated state as the groundwater level increases owing to rainfall infiltration. On the other hand, water movement on the surface of unsaturated soil is related to that in the saturated soil. To unify the two types of water movement means to address the so-called saturated and unsaturated seepage problem. Using hydraulic head  $h$  as the dependent variable, the anisotropic two-dimensional Richards saturated-unsaturated seepage control equation is as follows (Xiao SC et al., 2018; Hu XB et al., 2019; Yu GQ et al., 2015; Song DY, 2018):

$$\frac{\partial}{\partial x} k_x \frac{\partial h}{\partial x} + \frac{\partial}{\partial y} k_y \frac{\partial h}{\partial y} = m_w \rho_w g \frac{\partial h}{\partial t} \quad (1)$$

where  $k_x$  and  $k_y$  are the horizontal and vertical saturated permeability coefficients (m/s), respectively;  $\rho$  is the density of water;  $g$  is the gravitational acceleration;  $m_w$  is specific

water capacity, which is defined as the negative value of the partial derivative of the volumetric water content  $\theta$  with respect to the matrix suction ( $p_a - p_w$ ):

$$m_w = - \frac{\partial w \theta}{\partial (p_a - p_w)} \quad (2)$$

where  $p_a$  and  $p_w$  are the pore air pressure and pore water pressure, respectively.

#### 3.2. Engineering geological model for seepage simulation

In this paper, the authors established a seepage model by using SEEP/W and the Geo-slope software (Fig. 3) based on the main landslide section (Fig. 2).

The parameters in the model were obtained through tests and experience. The physical and mechanical parameters of each layer including permeability coefficients are shown in Table 1.

The boundary conditions of the model include: The boundary of the fixed head is below the groundwater level of the left and right sides in the model; the boundary of zero discharge is above the groundwater level, and the slope is the infiltration boundary condition (Li YY et al., 2020).

#### 3.3. Simulation conditions

Most daily precipitation caused by typhoons has been shown by previous studies to have a maximum of less than 200 mm in the southeastern coastal areas; it is attributable to the formation of approximately 88.4% of the typhoon events (Qiu WY et al., 2014; Figs. 3, 4). The critical daily precipitation required to trigger landslides is about 200 mm according to a recent statistical survey of landslide disasters induced by typhoons (Xie JM et al., 2003; Zhang SX et al., 2017; Zhang CY et al., 2019). For instance, a landslide disaster occurred after 195 mm of rainfall in 24 h on July 18, 2005 during Typhoon Haitang; a landslide disaster occurred after 290 mm of rainfall in 24 h on September 1, 2005 during Typhoon Taili. Therefore, in this paper, 200 mm/d is taken as the critical rainfall standard value that induces landslides to analyze the dynamic characteristics of hydrological changes in the landslide under typhoon-triggered rainstorm conditions. Transient seepage characteristics of the landslide are considered in the cases of successively increasing rainfall of 200 mm in 24 h and constant-intensity rainfall of 200 mm in 24 h (Iverson RM, 2000; Zhang W et al., 2019; Zhang M et al., 2019). The simulation duration was 24 h.

## 4. Numerical simulation

#### 4.1. Water seepage field in the landslide caused by a constant-intensity rainstorm

Fig. 5 shows the distribution of pore water pressure in the landslide slope during a constant-intensity rainstorm of 200

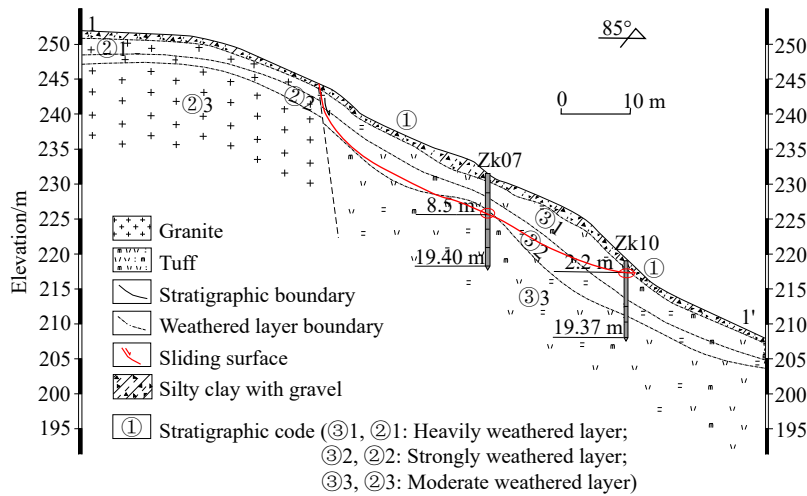


Fig. 2. Geological section of the Zhonglin Village landslide.

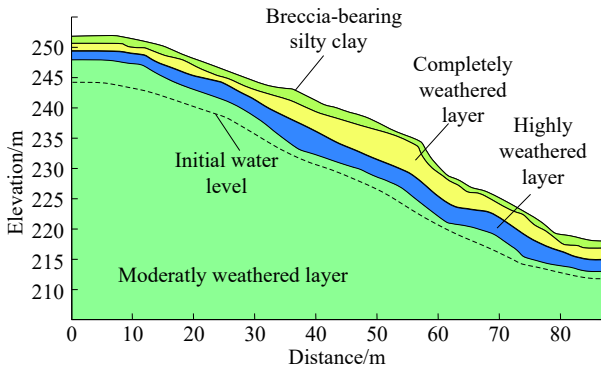


Fig. 3. Simulation model of layers in Zhonglin Village landslide.

Table 1. Physical and mechanical parameters used in the model.

Layer parameters	Breccia-bearing silty clay	Completely weathered layer	Strongly weathered layer	Moderately weathered layer
Natural unit weight $\gamma / (\text{kN/m}^3)$	18.7	19.3	20	25
Saturated volumetric moisture content /%	30	28	26	25
Saturated permeability coefficient/(m/h)	0.05	0.216	0.16	0.1
Cohesive force/c (kPa)	20.1	19	21	27
Internal friction angle/ $\varphi$ (°)	21.8	20	23	26

mm/d in 24 h. The seepage area is presented in blue color.

The simulation results in 4.8 h show that the groundwater level increased significantly, while the infiltration decreased gradually. This led to a decrease in the rise in groundwater level until a balance was reached (Figs. 5a, b), when the rate of the groundwater level rise stabilized at 1.04 m/h. After 4.8 h, heavy rainfall led to an accumulation of runoff. As a result,

the topsoil was saturated; a seepage face appeared in the shallow soil and then migrated slowly downwards (Fig. 5c), and differential infiltration occurred in some areas (Figs. 6d, 5e). After 24 h, the pore water pressure distribution shown in Fig. 5f. The hydrological response characteristics by this time are as follows. (1) The seepage face remained at the interface between the completely weathered soil (the second layer) and the highly weathered soil (the third layer). (2) The rock-soil above the seepage face was saturated. (3) The groundwater infiltration rate was 0.26 m/h. (4) All rainfall was converted to surface runoff; the soil erosion rate was increased. (5) The anti-shear performance of the rock-soil decreased. Consequently, a slide surface appeared at the interface between the completely weathered and highly weathered soil layer.

#### 4.2. Groundwater seepage field in the landslide caused by successively increasing rainfall

For the sake of comparison, the authors changed the rainfall model and introduced five successive 4.8 h rainfall intensities: 10 mm/d, 25 mm/d, 50 mm/d, 100 mm/d, and 200 mm/d (Fig. 6).

Fig. 7 shows the distribution of pore water pressure in the landslide slope during a successively increasing rainfall of 200 mm/d in 24 h. The seepage area is presented in blue color.

In this case, the groundwater level rose to its peak at 4.8 h and subsequently remained steady—similar to the case of constant-intensity rainfall according to the comparison of the groundwater level in Fig. 7 with that in Fig. 5. The silty clay layer on the landslide surface gradually developed into a seepage face as the rainfall intensity successively increased. Then the seepage face slowly migrated downwards at a rate less than that in the constant-intensity rainfall model. After 19.2 h when the rainfall reached 100 mm/d, the seepage face stabilized at the interface between the silty clay surface layer

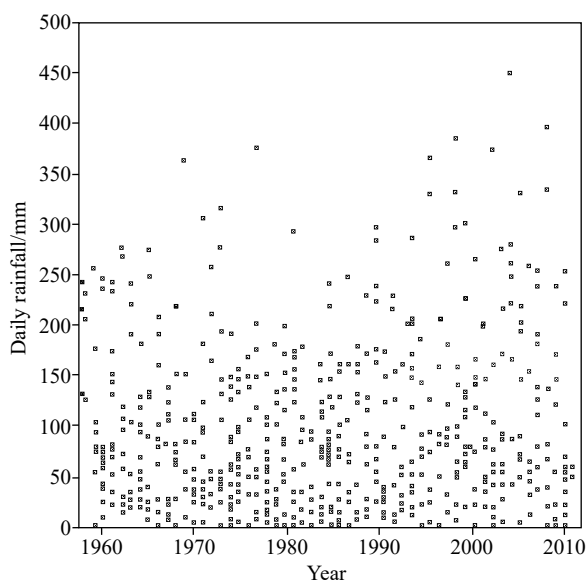


**Fig. 4.** Maximum daily typhoon-triggered rainfall from 1958 to 2012.

and the completely weathered layer; the slide surface formed in this case was shallower than that formed in the case of constant-intensity rainfall; the groundwater infiltration rate

was 0.16 m/h, and the all the rainfall was converted into surface runoff after 19.2 h. The water-induced softening and erosion of soil caused a shovel-shaped slope to develop.

**5. Conclusions**

The following conclusions can be drawn from this study:

(i) The influence of typhoon-triggered rainstorms on landslides can be divided into three main stages in the model. In the first stage, the groundwater level rose quickly and then stabilized within 4.8 h; the rock-soil beneath the groundwater level became saturated, and the water pressure continued to increase. In the second stage, surface runoff started to occur; a seepage face formed in shallow soil and then migrated downwards; the seepage face remained steady within 19–24 h; the rock-soil above the seepage face softened, and the anti-shear performance decreased. In the third stage, all the rainfall was converted into runoff; the surface rock-soil was strongly eroded, and the soil erosion rate increased.

(ii) In both of the aforementioned cases (constant-intensity rainfall and successively increasing rainfall), groundwater levels rose quickly. The rain infiltrated quickly and the water level rose rapidly within a short period of time (4.8 h) as the unsaturated soil has a high storage capacity and very large

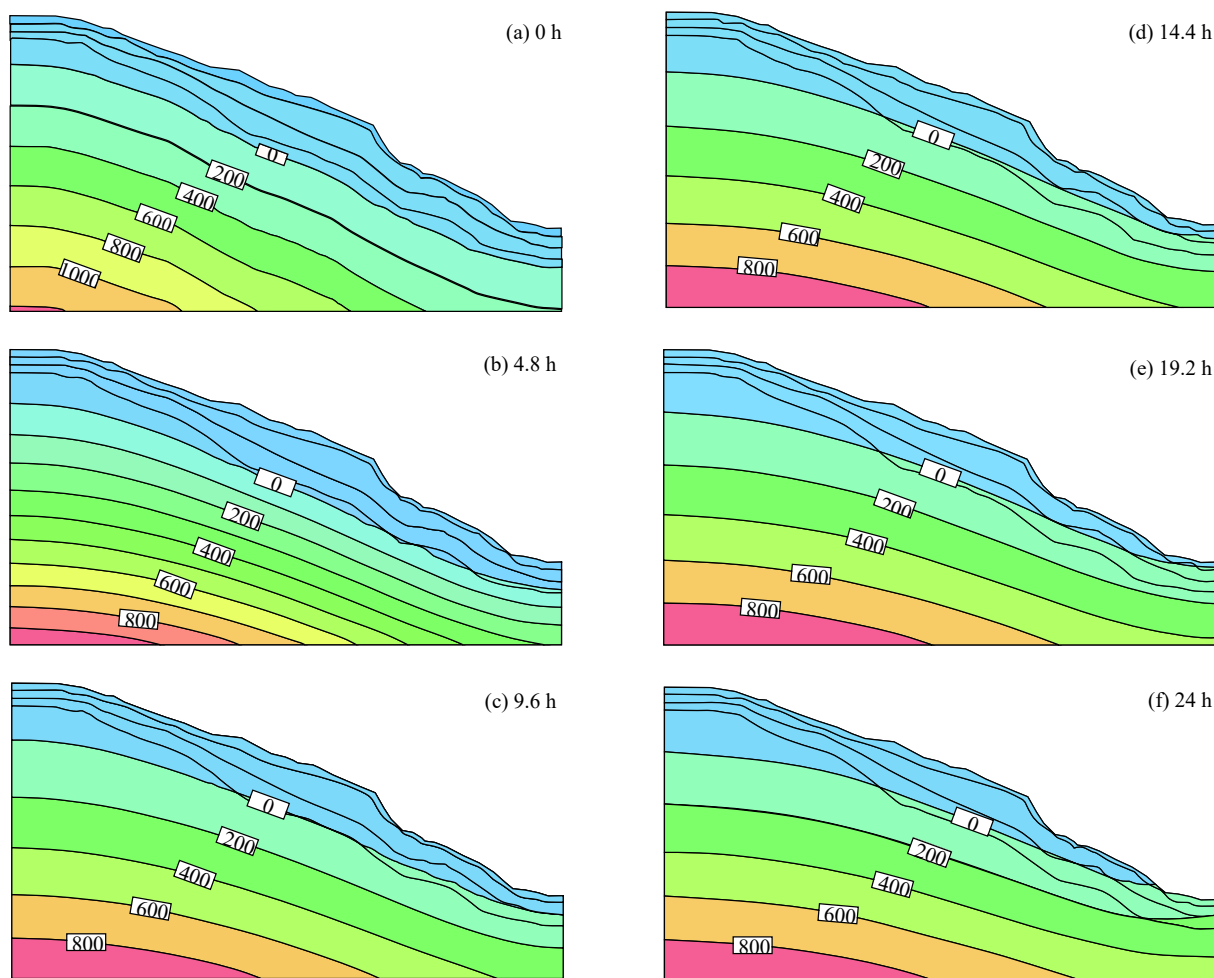


**Fig. 5.** Distribution of pore water pressure in the slope at different times during a constant-intensity rainstorm of 200 mm/d.

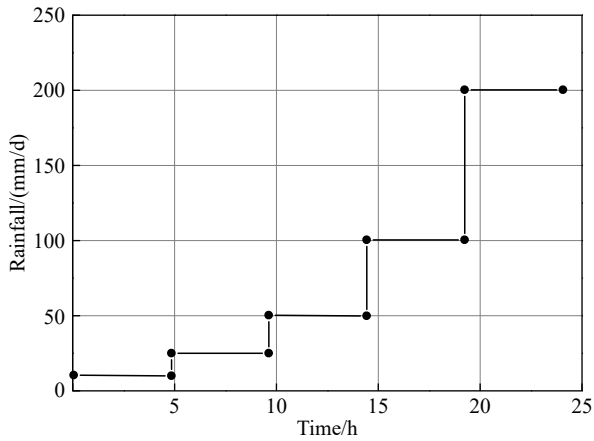


Fig. 6. Periods of successively increasing precipitation.

matrix suction. Then the groundwater level became stable owing to the increase in runoff.

(iii) The groundwater infiltration rate in a landslide is mainly affected by the intensity of typhoon-triggered rainfall: The higher the rainfall intensity, the larger the potential difference and the higher the infiltration rate. The simulation of Zhonglin Village landslide shows that constant-intensity

rainfall caused greater changes than the rainfall with successively increasing intensities, and constant-intensity rainfall generated deeper seepage face than successively increasing rainfall. Furthermore, the seepage face in the case of constant-intensity rainfall remained near the interface between the completely weathered layer and the highly weathered layer, while the seepage face in the case of successively increasing rainfall remained near the interface between the silty clay layer and the completely weathered layer.

(iv) The deformation mode of landslides is closely related to the intensity and duration of typhoon-triggered rainstorm. Constant-intensity rainfall is liable to induce deep landslides, with a burial depth of slip surface of greater than 2 m. In contrast, successively increasing rainfall tends to produce shovel-shaped slopes, whose burial depth is less than 2 m.

#### CRediT authorship contribution statement

Tai-li Zhang designed and performed the experiments, derived the models and analyzed the data. Qiang Sun and Sheng-he Wang assisted with the Zhonglin Village landslide measurements and Jian-bo Wu helped carry out the numerical simulation of the saturated-unsaturated seepage field of the

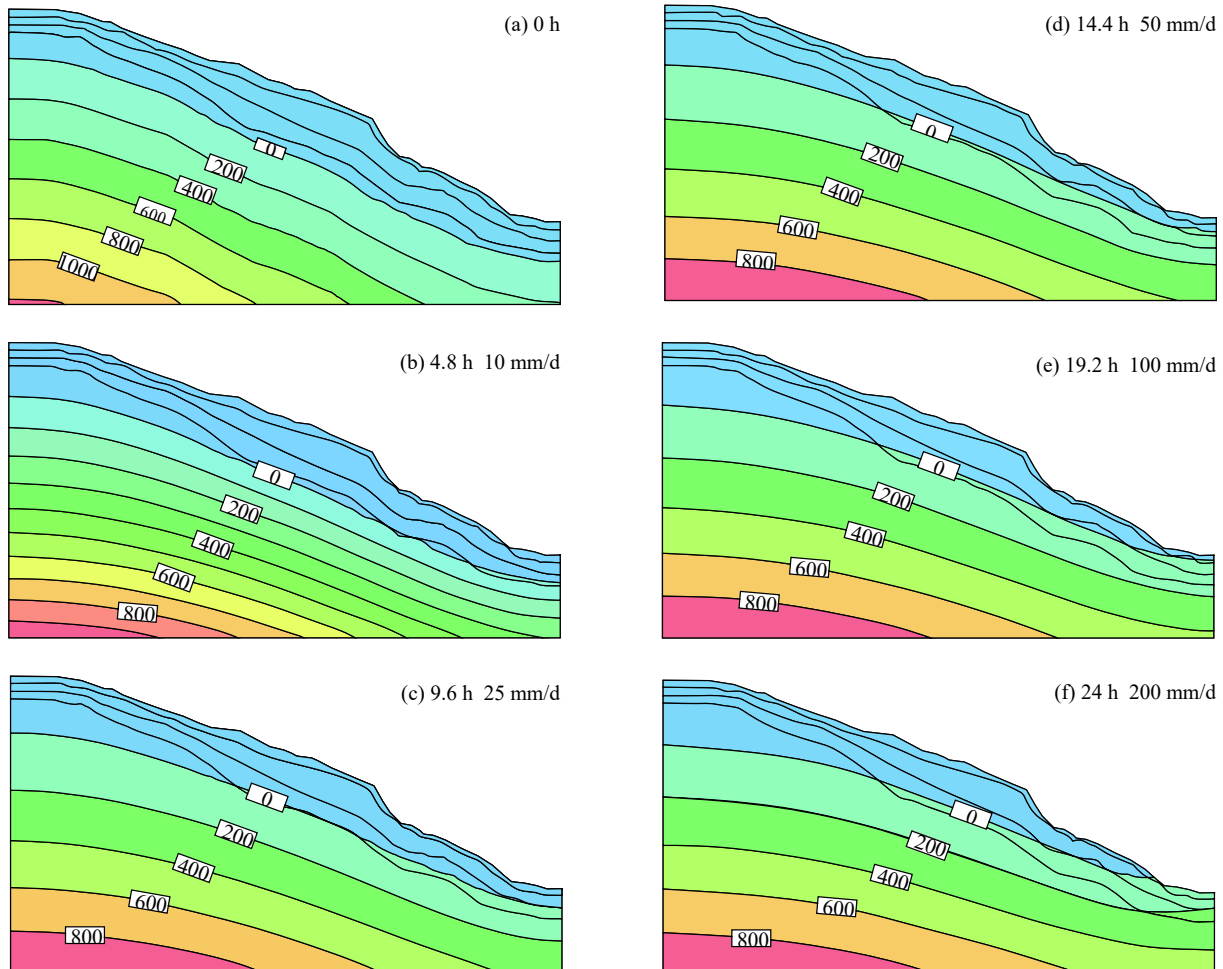


Fig. 7. Distribution of pore water pressure in the slope at different times in the case of successively increasing rainfall.

landslide under typhoon-triggered rainstorm conditions. Tai-li Zhang and Ai-guo Zhou wrote the manuscript in consultation.

### Declaration of competing interest

The authors declare no conflicts of interest.

### Acknowledgment

This work was supported by the Investigation Project of Geological Disasters in Feiyun Basin of Zhejiang Province (D20190648) and the Disaster Geological Survey Project of Lishui, Zhejiang Province (D20160282).

### References

- Chen GP. 2011. Study on Distribution Characteristics and Influencing Factors of Slope Geological Hazard Induced by Typhoon in Wenzhou. Chengdu, Chengdu University of Technology, Master's thesis (in Chinese with English abstract).
- Chen X, Liu JX. 2007. Analysis on Typhoon Catastrophe in Fujian, taking 200519# "Rongwang" Typhoon as an example. *Journal of Quanzhou Normal University (Natural Science)*, 25(2), 89–90 (in Chinese with English abstract).
- Han J. 2012. Physical Simulation Study on the Formation Mechanism of Typhoon Landslide in Wenzhou Region. Chengdu, Chengdu University of Technology, Master's thesis (in Chinese with English abstract).
- Hu XB, Fan XY, Tang JJ. 2019. Accumulation characteristics and energy conversion of high-speed and long-distance landslide on the basis of DEM: A case study of Sanxicun landslide. *Journal of Geomechanics*, 25(4), 527–534 (in Chinese with English abstract).
- Iverson RM. 2000. Landslide triggered by rain infiltration. *Water Resources Research*, 36(7), 1897–191. doi: [10.1029/2000WR900090](https://doi.org/10.1029/2000WR900090).
- Lou WP, Wu LH, Deng SR. 2006. Causes and characteristics of disasters of 0513 Typhoon Tali. *Journal of Catastrophology*, 21(2), 85–89 (in Chinese with English abstract).
- Li MB, Chen P, Chen ZH, Fang Q. 2019. Sensitivity zoning of rainfall-induced landslide hazard in Xuefeng Mountain area. *Geology and Resources*, 28(1), 78–84 (in Chinese with English abstract).
- Liu LL, Yin KL. 2008. Analysis of rainfall infiltration mechanism of rainstorm landslide. *Rock and Soil Mechanics*, 29(4), 1061–1066 (in Chinese with English abstract).
- Qiu WY. 2014. Characteristics of Tropical Cyclone Extreme Precipitation and Its Preliminary Causes in China's Southeast Coast. Nanjing, Nanjing University of Information Science and Technology, Master's thesis (in Chinese with English abstract).
- Qiao YX, Ma ZS, Lü FJ. 2009. Characteristics and dynamic cause mechanism of the Wenchuan Earthquake geological hazards. *Geology in China*, 36(3), 736–741 (in Chinese with English abstract).
- Song DY, Zhang MS, Mu HD, Wang W. 2018. Research on the evolution mechanism of deformation and failure of No.13 landslide in the north of Jiaojiaiatou. *Geological Bulletin of China*, 37(7), 1360–1364 (in Chinese with English abstract).
- Tang MG, Yang H, Xu Q, Fu XL, Zhu Q, Ma XJ. 2019. Permeability and parameters of landslide bodies in Three Gorges Reservoir area. *Journal of Engineering Geology*, 27(2), 325–332 (in Chinese with English abstract).
- Tan JM, Dong HG, Chang H, Han HQ, Zhang Y. 2018. Statistical analysis of the geological environment characteristics of landslide development in Qingjiang River Basin. *Geology and Mineral Resources of South China*, 34(4), 315–322 (in Chinese with English abstract).
- Wang JY, Wang GL, Shi XY. 2019. Mechanical analysis of apparent dip creep-buckling failure of Shanyang rockslide in Shaanxi Province. *Geology in China*, 46(2), 381–388 (in Chinese with English abstract).
- Xiao SC. 2018. Comparison of the landslide stability calculation and landslide stability evaluation method: A case of the cutting slope of a wind farm in Hengdong, Hunan. *Hydrogeology & Engineering Geology*, 45(3), 159–164 (in Chinese with English abstract).
- Xie JM, Liu LL, Yin KL. 2003. Study on the threshold values of rainfall of landslides hazards for early-warning and prediction in Zhejiang province. *Geological science and Technology Information*, 22(4), 101–105 (in Chinese with English abstract).
- Yu GQ, Zhang MS, Zhang CH. 2015. Numerical simulation for start-up of landslide based on continuum model. *Geological Bulletin of China*, 34(11), 2100–2107 (in Chinese with English abstract).
- Yin YP, Wang WP, Zhang N, Yan JK, Wei YJ, Yang LW. 2017. Long runout geological disaster initiated by the ridge-toprockslide in a strong earthquake area: A case study of the Xinmo landslide in Maoxian County, Sichuan Province. *Geology in China*, 44(5), 827–841 (in Chinese with English abstract).
- Yan YJ, Yan YS, Zhao GZ, Zhang TL, Sun Q. 2019. Study on moisture migration in natural slope using high-density electrical resistivity tomography method. *Rock and Soil Mechanics*, 40(7), 2807–2814 (in Chinese with English abstract).
- Li YY, Sheng YF, Chai B, Zhang W, Zhang TL, Wang JJ. 2020. Collapse susceptibility assessment using a support vector machine compared with back-propagation and radial basis function neural networks. *Geomatics, Natural Hazards and Risk*, 11(1), 510–534. doi: [10.1080/19475705.2020.1734101](https://doi.org/10.1080/19475705.2020.1734101).
- Zhou CB, Li DQ. 2009. Advances in rainfall-induced landslides mechanism and risk mitigation. *Advances in earth science*, 24(5), 477–487 (in Chinese with English abstract).
- Zhang CY, Zhang TL, Zhang M, Sun Q, Wu JB, Wang HS. 2019. Rainfall infiltration characteristics and numerical simulation of slope instability in the basalt residual soil in the coastal area of Southeast China. *Hydrogeology & Engineering geology*, 46(4), 42–50 (in Chinese with English abstract).
- Zhang SX, Yang WM, Cheng XJ, Tian Y, Li H, Huang Y. 2017. Genetic mechanism and stability analysis of loess landslides group in Tianshui Hongqishan, Gansu Province. *Geology in China*, 44(5), 924–937 (in Chinese with English abstract).
- Zhang W, Li YY, Zhang TL, Gui L, Zhou C. 2019. Remote sensing interpretation of landslide geological hazards in high vegetation coverage area based on hazard sensitivity analysis. *Safety and Environmental Engineering*, 26(3), 28–35 (in Chinese with English abstract).
- Zhang M, Yang L, Ren XW, Zhang CY, Zhang TL, Zhang JJ. 2019. Field model experiments to determine mechanisms of rainstorm-induced shallow landslides in the Feiyunjiang River basin, China. *Engineering Geology*, 262, 1–9.